EFFECT OF DIFFERENT INTAKE SHAPES ON THE FLUID FLOW CHARACTERISTICS OF A RIBBED RECTANGULAR DUCT

A. A. Abdel Aziz[*]; K. A. Mahmoud[**]; K. M. El-Shazly[***]; M. F. Abd Rabbo[***]

[*] lecturer, Faculty of Eng. Shoubra, Benha Branch, Zagazig University
[**]lecturer Assistance, Faculty of Eng. Shoubra, Benha Branch, Zagazig University
[***] Profs., Faculty of Eng. Shoubra, Benha Branch, Zagazig University

ABSTRACT

The developing region was investigated experimentally in this paper for smooth and ribbed duct to enhance the heat transfer coefficient at equal pumping power constraint through the flow passage. The mean velocity of air stream varies from about 4 to 18 m/s corresponding to a range of Reynolds number from 1.62 x 10^4 to 7.2 x 10^4, the rib pitch- to- height ratio (P/e) varies from 10 to 20, the rib height-to channel hydraulic diameter ratio (e/D_e) is fixed at 0.081, and the channel length to hydraulic diameter ratio (L/D_e) is fixed at 18.75. A rectangular channel with an aspect ratio (W/H) of 4:1 ribbed with square ribs is investigated at different intake shapes (bellmouth, plenum box, and abrupt intakes). The effects of the different investigated parameters on the local and average static pressure, and friction factor are studied. For smooth duct with abrupt and plenum intakes, the maximum static pressure coefficient was found at the reattachment point at about X/D_e=0.95, while it was found at X/D_e=0.17 for bellmouth intake. For ribbed duct the effect of the intake shape becomes more significant at the entrance region (X/De<0.69). For the ribbed duct with the abrupt intake it was found that the static pressure coefficient (Cp) is lower than that of plenum and bellmouth ribbed ducts. These may be attributed to that the abrupt intakes improve the flow pattern (turbulent and acceleration) in the entrance region more than that for plenum and bellmouth. The average static pressure coefficients (Cp) for abrupt and plenum intakes are lower than that for bellmouth intake for smooth and ribbed wall and it were independent of Reynolds number for Re>40,000. Good agreement was found between the experimental results and [Liou, et. Al., 1992] data for direct comparison of static pressure for ribbed duct with plenum intake. The experimental correlations of the average static pressure coefficient (Cp) for the developing region of a ribbed duct with different intake shapes are obtained.

$$Cp_{average} = a\ Re^{b}\ (P/e)^{c} \qquad (1)$$

The constant coefficients (a, b, c) and the relative error are listed in table 2. Flow visualization results were carried out to support the measured results and illustrate the flow characteristics around the intake and the ribs.

KEYWORDS: Entrance region, Intake shape, Ribbed duct, Fluid Flow, Flow visualization.

ملخص البحث

لتحسين معامل انتقال الحرارة خلال مسلك تبريد داخلى لريشة تربينة ، تم عمل دراسة لخصائص السريان عند منطقة الدخول لهذا المسلك. حيث تم عمل محاكاة لمسلك تبريد داخلى لريشة تربينة مزود بعروق ذو نسبة باعية تساوى 4 وذلك عند ثلاثة أشكال مختلفة للمدخل وهم صندوق تجميع ، مدخل حاد ، و مدخل ذو شكل فوهة الجرس ، وكان مدى عدد رينولدز من 16200 إلى 72000 ، ونسبة خطوة العرق إلى ارتفاعه 10 و 20 . تم دراسة تأثير المتغيرات السابقة على معامل الضغط الاستاتيكى الموضعى والمتوسط ومعامل الاحتكاك. فى حالة مسلك بدون عروق وذو مدخل تجميع ومدخل حاد وجد أن أقصى معامل ضغط استاتيكى يحدث عند X/D_e=0.95 ، وعند X/D_e=0.17 بالنسبة لمدخل ذو فوهة جرس وذلك عند نقط إعادة الارتطام مع سطح المسلك . المدخل الحاد يسبب أقل معامل ضغط أستاتيكى إذا ما قورن بالمداخل الأخرى ،

1. INTRODUCTION

The effect of rough surface on the fluid dynamics and heat transfer in turbulent flow have been intensively studied last few years due to the importance of these studies in design of turbine blades cooling passage, gas cooled reactors, and also compact heat exchanger. In all these applications the heat transfer exchanging length is short so that the developing length (hydraulic and thermal) has a strong effect on the overall heat transfer coefficient. Therefore, the present work is directed to study fluid flow characteristics through the entrance length of roughened ducts.The effect of different parameters on the heat transfer and fluid flow characteristics, which neglect the effect of the entrance shape, was extensively investigated by many of the previous investigations. This entrance shape may strongly affect the heat transfer and fluid flow in the short developing length. In the developing length the relevant parameters in the previous work were the different rib pitches and Reynolds numbers for plenum intake [Liou, et. al., 1992], the different entrance shapes for circular tube [Kays, et. al., 1980], different aspect ratios and pitch to height ratios for plenum intake [Han, et. al., 1988], detached and attached ribs for plenum intake [Liou, et. al.,1995] and [Tsia, et. al.,1999]. Rectangular duct with bellmouth and sharp edge intakes [Hirota, et. al.,1990], and large aspect ratio for symmetric and asymmetric heating duct with abrupt intake [Sparrow, et. al., 1983]. Therefore, in the present paper the effect of the different intake shapes on flow characteristics for the smooth and roughened rectangular duct is investigated. The main objective of the present work is to study the effect of the following parameters on the fluid flow characteristics in the entrance region: the entrance shape, the rib pitch to the height ratio (P/e), and Reynolds number. Table 1 shows briefly the intake shapes and rib pitches used in the present study.

TABLE 1: Intake duct shape, and rib pitches used in the present experimental work.

Intake Shape	P/e	Shape
Bellmouth	Smooth	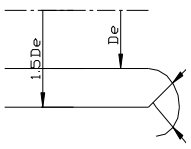 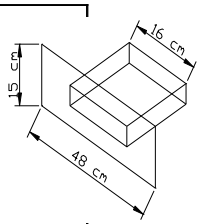
	10	
	20	
Plenum	Smooth	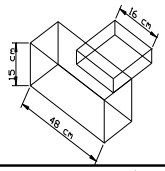
	10	
	20	
Abrupt	Smooth	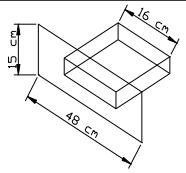
	10	
	20	

2. EXPERIMENTAL SETUP

The study of turbulent flow characteristics through a roughened duct in two channel models is the objective of the present work through the developing length. A special test section was built up to perform flow measurements in the duct, and a special simulated model was built up also, for flow visualization. The flow system consists of: suction air blower, flow orifice, transition duct, straightener, test section with different intake shapes. A long calming section was used between the blower intake and the rectangular cross section. The schematic diagram of channel flow system is shown in Fig. (1). The airflow discharge is controlled at the outlet of the air blower by means of a variable area outlet gate.

2.1 Test Section

The test section is a horizontal rectangular duct having dimensions 160x40 mm. The channel of aspect ratio 4:1 used in this paper is the same aspect ratio employed by most of the previous work as for example in [Abd El-Aziz 1999], [Liou et.al.,1992] and [Han et.al.,1988]. The test section is 1200 mm in length and has a rectangular cross section 160 mm x 40 mm (Plexiglas sides). Aluminum square ribs with height of 5.2 mm are placed on each of the principal wall at different pitches. Construction details of the test section and of the different intake shapes are shown in Fig.(2). Test section is constructed with the two principal walls made of Plexiglas plate 8 mm thickness. Pressure taps were distributed along the developing and fully developed region of the test section. For rib pitch to height ratio of 10 there are 7 pressure taps distributed along 45 mm (one in the middle distance of rib pitch, two spaced at 5 mm from each side, two spaced at 6.5 mm from the previous, two spaced at further 10 mm). In the fully developed region after 7 pitches the number of the pressure taps is reduced to 65 pressure taps. A digital Micro-Manometer is used to measure the differential pressure. Check of the span-wise distributions of the air pressure across the test section width were measured at different values of Reynolds number. The results are shown in Fig.(3) for ribbed duct with pitch to height ratio (P/e = 20). A maximum deviation of average pressure in the span-wise direction was observed about 4%.

In order to find the qualitative characteristics of the flow field around the intake shapes and the ribs, a smoke visualization technique is employed in a smoke tunnel. The smoke tunnel is used to view flow patterns, recirculation, separation, and reattachment point down stream of the intake and around the ribs. The smoke tunnel consists of a suction fan with a variable speed mounted on the top of the tunnel and the test section of 180 (width) x 240 (height) x 100 (depth) mm. Uniform streamlines of smoke are driven vertically upwards to the test section by the suction fan. Kerosene-vapor is generated in glass bottle by an electric heater. Ribbed-wall models with different intake shapes are attached to the rear wall of the working section while the front wall is of Plexiglas and movable. The smoke is driven upwards to the test section by the suction fan from

a muslin strainer at the bottom section. A smoke rake is located below the working section, which emits twenty-three streams of smoke introduce smoke. The free-stream velocity of smoke is changed from a 1 m/s to about 3 m/s by a voltage regulator. The working section is brightly illuminated from both sides and the flow pattern is clearly visible. A sensitive camera is used to view the flow pattern through the test model with different intakes with short focus distance to allow to capture clear photographs.

3. EXPERIMENTAL RESULTS

To confirm the validity of the present measurements, the friction factor for smooth duct was compared with White's equation Eq.(2) Ozisik[10] for the fully developed flow in smooth pipe and the results are shown in Fig. (4). The friction factor results of the rectangular duct with an aspect ratio (AR=4) are slightly higher than those of previous results ([8] and [9]). This difference is due to the duct aspect ratio of AR=4.

$$f_s = 0.316 \times Re^{-0.25} \qquad (2)$$

A correction factor $K_{correction}$ for the rectangular duct with different height to width ratios (H/w) was cited in Abd El-shahed, et. al., 2003[9] and its value varying from 1.097 for (H/w=0.0) to 1.0 for square duct (H/w=1.0).

$$K_{correction} = 1.097 - 0.177 \times (H/w) + 0.083 \times (H/w)^2 \qquad (3)$$

where,

$$K_{correction} = f_{Rect} / f_s \qquad (4)$$

The static pressure through the mid-span of bottom wall of channel was measured and the static pressure coefficient (Cp) was obtained.

$$Cp = (p_x - P_\infty)/(0.5\rho u_m^2) \qquad (5)$$

The static pressure distributions along the ribbed duct bottom wall for the developing length were measured by seventy-three pressure taps. The static pressure distribution was measured in the developing length by a dense distribution of the pressure taps and in the fully developed region by a little number of pressure taps. The present experiments were carried out at two different pitches to height ratio of (10 and 20), for a fixed e/H ratio of 0.081, within a range of Reynolds number from 1.62 $X10^4$ to 7.2 $X10^4$.The friction factor in the fully developed region was calculated from the pressure drop across the flow duct evaluated by taking the pressure gradient between two consecutive points of successive cycles to the rib pitch.

$$f = \{(\Delta P/\Delta X)D_e\}/(0.5\rho U_m^2) \quad (6)$$

Figure (5 a, b, c) shows the static pressure coefficient axial distribution for a roughened duct with square ribs at P/e=10 for different intake shapes, and Reynolds numbers. For bellmouth intake it was found that the maximum static pressure coefficient occurs at entrance till X/D=0.69, upstream the first rib directly, and then decreases suddenly where the flow is accelerated due to the blockage effect and boundary layer distortion. For plenum and abrupt entrance shapes it was observed that the static pressure have the same trend as for bellmouth intake, this is due to the dominant effect of the ribs. It can be concluded that the entrance shape can distort the boundary layer and accelerate the flow with the same extent as the blockage effect of ribs but with less pumping power. These results were confirmed by flow visualizations. Figure (6 a, b, c) shows the static pressure for roughened duct with square ribs at P/e =20 , for different intake shapes, and Reynolds numbers. Figures (5) and (6) show that for Re>40,000 there is no significant effect of Reynolds number on the static pressure coefficient. It was noticed that for plenum and abrupt intakes, flow separates at duct inlet immediately. The static pressure decreases slowly from entrance and the reattachment point appears at X/D_e of about 0.27 and 0.53 for bellmouth and (abrupt and plenum) intakes, respectively. For the bellmouth intake, there was a direct increase in Cp from inlet till the position of the first rib. This was observed by the flow visualization. The static pressure coefficient downstream of the reattachment point increases till it reaches a peak value at about X/D_e=1.46 from the intake and then decreases due to the blockage effect of the roughened duct. Figure (7) shows intake shape effect on the static pressure coefficient for smooth duct at constant Reynolds number. It was found that the static pressure coefficient for bellmouth intake is higher than for the plenum and the abrupt intakes. Also, it was observed that the maximum value of static pressure coefficient occurs at a distance of about X/D_e=0.17 for smooth intake (bellmouth) while it is shifted to X/D_e of about 0.95 for both the plenum and abrupt intakes. The results show that the plenum and abrupt intakes significantly affect the flow characteristics through the developing length. The static pressure coefficients for the plenum and abrupt intakes are smaller than that for bellmouth intake, this is due to the flow acceleration at the entrance.

Figures (8) and (9) show the static pressure distribution for roughened duct with square ribs at P/e=10 and P/e=20, respectively, with different intake shapes at Re=55,650. It was observed that at the entrance region of the duct (X/D_e< 0.68), the abrupt and plenum intakes have lower values of Cp compared with bellmouth intake. The effect of the intake shape is more significant upstream of the first rib at X/D_e<1.46 for P/e=20 and the static pressure for the bellmouth intake is clearly observed to be greater than that for the plenum and abrupt intakes. Therefore, the entrance shapes affect much the Cp in the entrance region (X/D_e< 0.69). This means that the flow acceleration and boundary layer distortion are existed due to the effect of entrance shapes for (X/D_e< 0.69) while the blockage effect due to

ribs dominates for (X/D_e> 0.69) downstream the first rib. This improves the heat transfer at both entrance and fully developed regions.

Figures (10), (11), and (12) show the variation of static pressure coefficient for different rib pitches, for bellmouth, plenum, and abrupt intake shapes at Re=55,650. The static pressure have the same fashion for the different rib pitches, and intake shapes. It was noticed that for P/e=10 the static pressure upstream region of the first rib is higher than those for each of P/e=20 and the smooth duct. Also, the static pressure for P/e=10 is lower than that for the P/e=20 and for smooth duct at X/D_e>1. It was found that, at P/e=10, the rib effect appears (beyond X/D_e=0.27) this is due to the blockage effect where the boundary layer is no longer able to growth up due to presence of ribs. The static pressure for smooth duct have larger values than that for the ribbed duct with P/e = 10, 20 downstream the first rib location. Flow acceleration through the ribbed duct reduces the static pressure compared with that for the smooth duct. Also, the formation of thick boundary layer for smooth duct increases the static pressure coefficient rather than that for ribbed wall duct. It was observed from Fig. (10) that the smooth duct and the ribbed duct with P/e=10 and 20 have nearly the same static pressure coefficient for X/D_e<0.27.The static pressure coefficient increases sharply to a peak value for X/D_e>0.27 and X/De>0.95 for ribbed duct with P/e=10 and 20, respectively. For P/e=20 the boundary layer growth up with a greater rate than that for the P/e=10 upstream the first rib.

The average value of static pressure coefficient ($Cp_{average}$) at different Reynolds numbers and intake shapes was calculated by integrating the local static pressure coefficients. Figure (13) shows the average static pressure coefficient ($Cp_{average}$) versus Reynolds number for a smooth duct with different intake shapes. It was observed that the average pressure coefficient for abrupt and plenum is less than that for the bellmouth intake in general. For smooth duct, the average pressure coefficient ($Cp_{average}$) strongly depends on the intake shape while it is independent of Reynolds number specially for Re>40,000. The sharp intakes (plenum and abrupt) accelerate the flow where a high velocity exists downstream the entrance that generates a high negative static pressure coefficients. Figure (14) shows the variation of average static pressure ($Cp_{average}$) through a roughened duct with square ribs at P/e = 10 and 20 , respectively, for different intake shapes. Low values of the $Cp_{average}$ occur more likely for roughened duct with square ribs than that for smooth duct. The average static pressure decreases as the Reynolds number increases. Abrupt and plenum intakes have lower values of static pressure than that for the bellmouth intake for different values of Reynolds number and rip pitch. The abrupt and plenum intakes generate vortices directly downstream the entrance edge and as a result the flow becomes more turbulent which is required to enhance the heat transfer at developing region. It can be observed that due to a sudden contraction in flow duct area (for abrupt and plenum intakes), a flow pattern is improved where the flow is accelerated and becomes more turbulent at entrance. For high value of Reynolds number (Re>40,000), the average static pressures have nearly a

constant value and the trend tends to a horizontal line for P/e=20. These results illustrate that there is no significant effect of Reynolds number on the average static pressure when (Re>40,000). The present results of local static pressure coefficient were compared with that of Liou [1] who studied the local static pressure distribution along the axial dimensionless (X/D_e) distance for plenum intake and square rib with P/e = 10 and 20 and at constant Reynolds number (Re = 33,000). It was observed from Figs.(15), and (16) that the present results are in good agreement with Liou's data[1] for the plenum intake for a range of Reynolds number from 17,000 to 40,000.

3.1 Friction Factor

Figure (17 a, b) shows the friction factor ratio (f/fs) versus Reynolds number in the fully developed region for roughened duct with different rib pitches and intake shapes. The friction factor ratio is independent of both the intake shape and Reynolds number for Re > 40,000. It was noticed from Fig. (18) that for the smooth duct, White and corrected equations have lower values of friction factor than those of the roughened duct. It was observed that as the Reynolds number increases from 20,000 to 40,000, the friction factor decreases slowly and then it approaches to a horizontal line. Figure (18) shows the friction factor for roughened duct with bellmouth intake and square ribs, for the two pitches to height ratio (P/e=10,20). It was found that friction factor for P/e=10 is greater than that for P/e=20 in general.

3.2 Flow Visualization Results

The flow patterns around the ribs and at entrance of the roughened duct are visualized by a flow visualization technique in a smoke tunnel. The stagnation zone exists on the front face of ribs and the flow patterns at the entrance are viewed by smoke tunnel. The smoke visualization experimental tests are carried out through channels with different entrance shapes (bellmouth, plenum, and abrupt) and rib pitches (10 and 20).

To determine the size and shape of flow zones caused by intakes and ribs, the test models were used with a height of 40 mm similar to the test duct height. Figure (19) shows the flow patterns through roughened channels with two-ribbed walls with square ribs (P/e = 10 and P/e=20) for different intake shapes. It was quantitatively observed that the square ribs will affect flow patterns. For P/e = 10, the flow reattaches to the downstream ribbed-wall of channel at an impingement point at distance of (5e) downstream the rib, generating a recirculation zone. The recirculation flow zone downstream the ribs are enlarged strongly than that downstream the plenum and abrupt intakes for (P/e=10) due to the blockage effect.

The recirculation zone downstream the channel intake is extended obviously as the rib pitch increases from P/e=10 to P/e=20. The downstream rib has no

significant effect on the flow patterns (separation, recirculation, and reattachment) caused by the abrupt and plenum intake shapes and this effect is diminished for P/e>10. The wake region downstream the intake becomes highly turbulent with a low velocity. These recirculation flow zones depend on the intake shapes. Therefore the intake shapes generally have an effect on the flow patterns and can alter the recirculating zone specially on the upstream region of the first rib. This may lead to an enhancement in the heat transfer rate for the abrupt and plenum more than that for the bellmouth. The effect of the intake shape shows that for the abrupt and plenum intakes the wake region formation extended obviously compared with that caused by the bellmouth intake due to the sharp edge intake. It was observed that a cyclic periodic of flow pattern happened next to the first rib and between the successive rib pairs.
For different intake shapes and Reynolds numbers, the present experimental data for the average static pressure coefficient ($Cp_{average}$) were correlated and the constants (a, b, c) of the following correlation were obtained for the different intakes and different rib geometries :-

$$Cp_{average} = a\ Re^{\,b}\ (P/e)^{\,c}$$

Table (2) Lists the constant coefficients for equation (1).

Constants	Intake shapes		
	Bellmouth	Plenum	Abrupt
a	-0.025	-0.060	-0.098
b	0.470	0.422	0.348
c	-0.184	-0.274	-0.171
Max error %	7.1	6.7	6.4

4. Conclusions

The experimental and the flow visualization result for the duct with opposite ribbed walls with different rib pitches and intake shapes are concluded as follows:

1. The local and the average static pressure coefficients for sharp intakes (abrupt and plenum) for both smooth and ribbed ducts are lower than that for bellmouth intakes in the developing length.

2. For smooth duct with abrupt and plenum intakes the maximum static pressure coefficient occurs at X/D_e=0.6 due to flow reattachment, and that for bellmouth at X/D_e=0.17.
3. Reynolds number does not affect the local static pressure coefficient for different intake shapes for smooth and ribbed duct. The effect of Reynolds number appears only at lower Reynolds numbers Re<36,800.
4. The local static pressure coefficient Cp for P/e=10 is lower than that for P/e=20.
5. The average static pressure decreases with the increase in Reynolds number (Re) and the value of the average static pressure coefficient $Cp_{average}$ is independent of Reynolds number.
6. The average static pressure coefficient increases with the rib pitch for different rib geometries.
7. The intake shapes have no significant effect on the friction factor.
8. Friction factor for P/e=10 is larger than that for P/e=20 with about 20% to 31%.
9. The flow visualization results are in phase with the experimental results, giving good viewing for the separation and reattachment points.

NOMENCLATURE

a. - rib width, mm
b. - rib width, m
Cp - static pressure coefficient $C_p = (p_x - P_\infty)/(0.5\rho u_m^2)$
$Cp_{average}$ - average static pressure coefficient
D_e - equivalent hydraulic diameter, m
e. - rib height, m
e/D_e - rib height to the equivalent hydraulic diameter
f - average friction factor
$f = \{(\Delta p/\Delta x)D_e\}/(0.5\rho u_m^2)$
f_s - smooth circular tubes friction factor
g - gravity, m/s^2
H - channel height, m
h - heat transfer coefficient, $W/m^2.K$
L - test channel length, m
L/D_e - test channel length to hydraulic diameter
m. - mass flow rate of air flow, kg/s
P - rib pitch, m, pressure, Pa
P/e - rib pitch to height ratio (distance between successive ribs per rib height
p_∞ - ambient static pressure , Pa
P_{st} - static pressure at the span wise midpoint of duct bottom plate
P_x - local static pressure distributions at centerline of ribbed-duct, Pa

Δp - pressure drop across the flow channel, Pa
$\Delta p/\Delta x$ - axial pressure gradient evaluated by taking the ratio of pressure drop between two consecutive points of successive cycles to the rib
pitch we take between the rib number 11,13.
t - time, Sec.
u_m - axial mean velocity, m/s
W - channel width, m
W/H - channel aspect ratio width to height of the duct.
X - axial distance, m
Δx - axial distance, m
z - spanwise coordinate, m

Greek Symbols

μ - viscosity, Kg/m.s
τ - shear stress, kg/m.s^2
ν - kinematics viscosity, m^2/s
ρ4 - density, kg/m^3
Δ - difference

Subscripts

b - bulk
d - dynamic
e - equivalent
h - value at leading edge of heated duct
in - inlet
r - ribbed-wall
st - static
s - smooth
t - total
w - wall
x - local distance in the axial direction of the duct at mid point span direction

Abbreviations

AR - channel aspect ratio, (W/H)

REFERENCES

1. Liou, T. M., Hwang, J. J., " Developing heat transfer and friction in a ribbed rectangular duct with flow separation at inlet" Journal of Heat transfer, Vol. 114, pp 565-573, 1992
2. Kays, W. M., and Crawfold, M. E.," Convective heat and mass transfer " 2nd ed., p.311-353 McGraw-Hill, 1980
3. J. C. Han " Heat transfer and friction characteristics in rectangular channels with rib turbulator" Journal of Heat transfer, Vol. 110, pp 321-328, 1988
4. Liou, T. M., Wang, W. B., " Laser holographic interferometry study of developing heat transfer in a duct with a detached rib array" Int. J. Heat and Mass transfer Vol. 38, No. 1, pp. 91-100, 1995
5. J. P. Tsia, J. J. Hwang " Measurement of heat transfer and fluid flow in rectangular duct with alternate attached-detached rib-arrays" Int. J. Heat and Mass transfer Vol. 42, pp. 2071-2083, 1999
6. M. Hirota, H. Fujita, H. Yokosawa, and T. Nonogawa, " Experimental study on mass transfer in the entrance region of rectangular duct" Department of Mechanical Eng. Nagoya University, Chikusa.ku, Nagoya 464-01, Japan,1990.
7. E. M. Sparrow, N. Cur, " Turbulent heat transfer in symmetrically or asymmetrically heated flat rectangular duct with flow separation at inlet" Transaction of the ASME vol. 104, pp. 82-89, 1983
8. A. A. Abdel Aziz, "Experimental and Numerical study of turbulent flow and heat transfer within a rectangular duct with different rib shapes" A thesis submitted to the faculty of engineering Shoubra-Zagazig university, mechanical engineering department for the degree of doctor of philosophy in mechanical engineering, 1999.
9. S. M. Abd El-Shahed "Thermo hydraulic behavior of research reactor and design base accidents" A thesis submitted in fulfillment to the faculty of engineering Shoubra-Zagazig university mechanical engineering department for the degree of master of science in mechanical engineering, 2003.
10. Ozisik, M. Necati, "Heat Transfer," McGraw-Hill, Co-singapore, 1985.

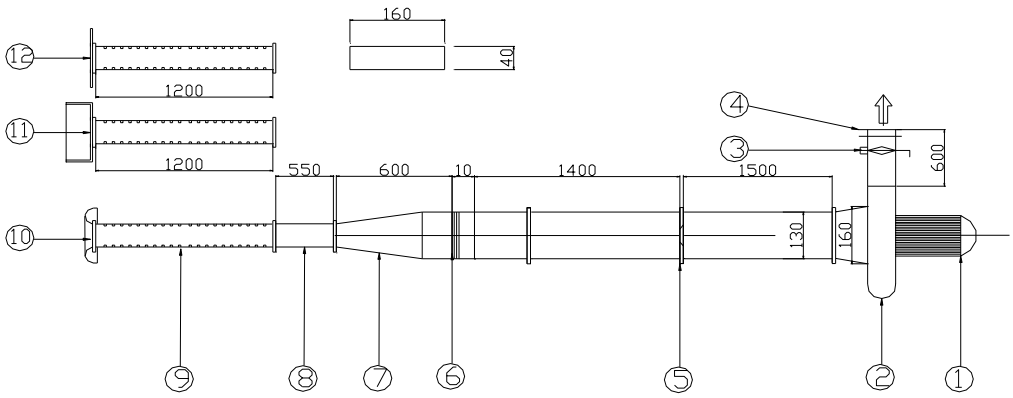

1-	1- A.C electric motor 3 Hp power	7-	Transition duct.
2-	2- Air blower	8-	Exit duct.
3-	3- Air gate controller (Volume damper).	9-	Test section.
4-	4- Exit duct.	10-	Duct with bellmouth intake.
5-	5- Flow orifice meter	11-	Duct with plenum intake.
6-	6- Straightener.	12-	Duct with abrupt intake.

Dimensions are in mm

Fig (1) Schematic diagram of the test rig.

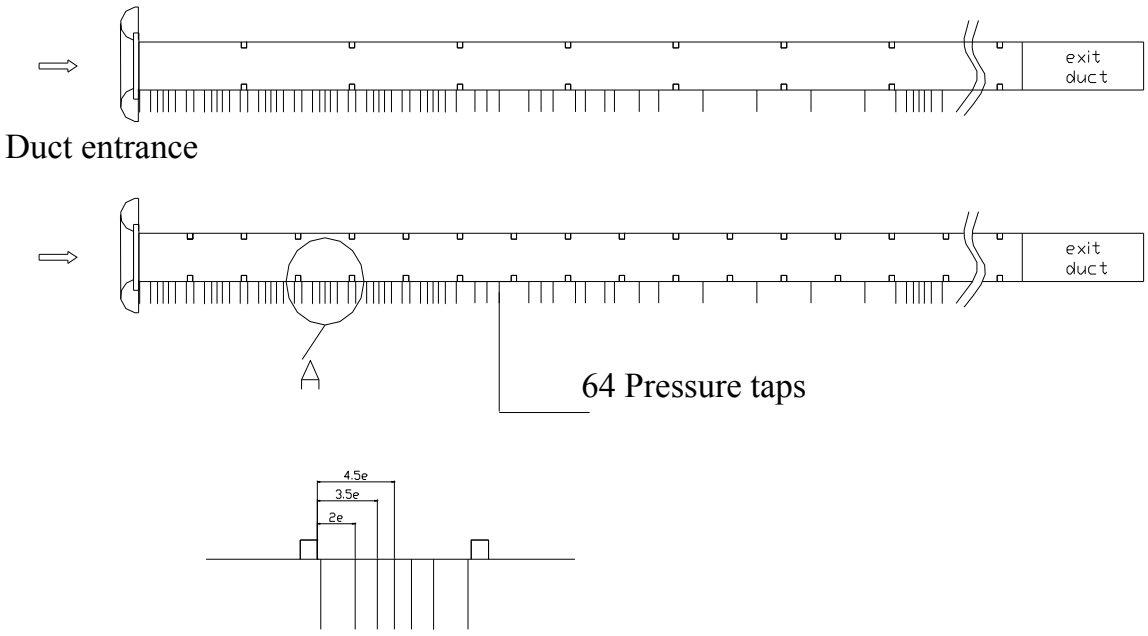

View (A)

Pressure taps locations along the test sections.

Fig.(2) Test sections details for hydrodynamics measurements.

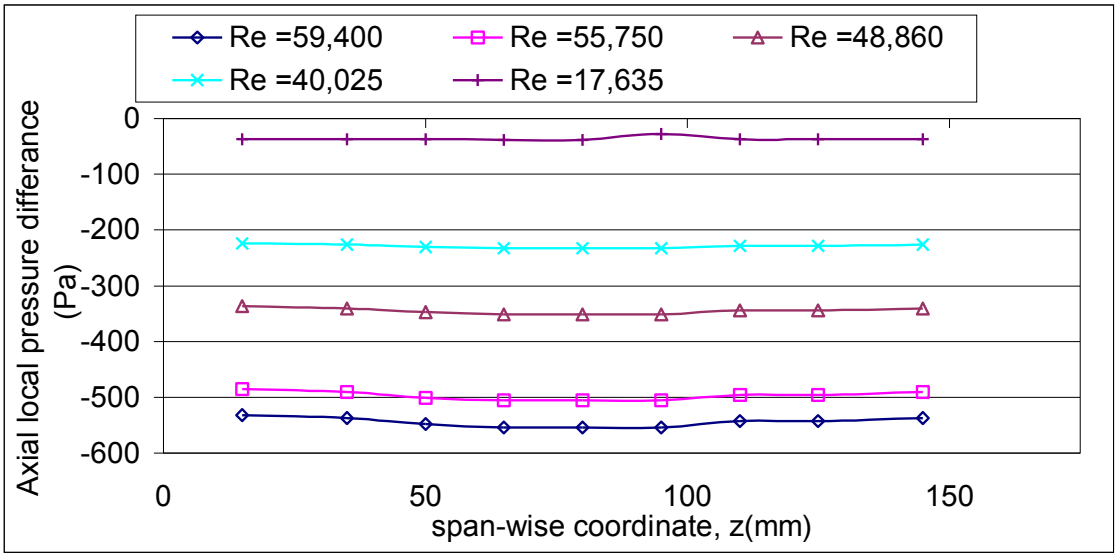

Fig.(3) Span-wise distribution of axial local pressure at various Reynolds numbers for square ribbed duct with P/e = 20.

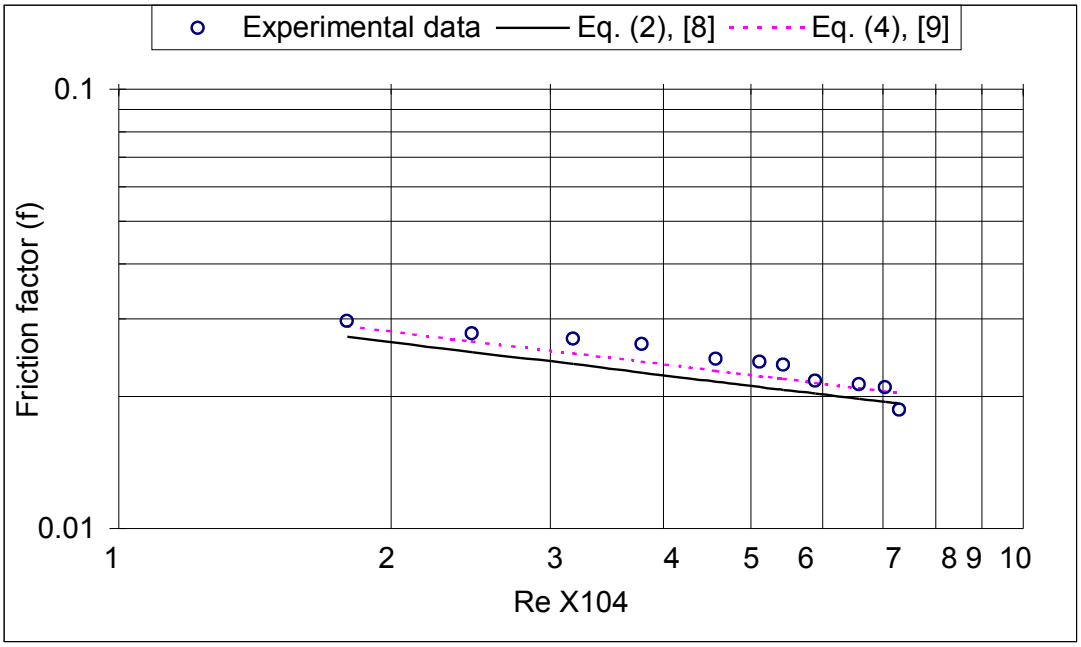

Fig.(4) Comparison of the present work experimental data for friction factor for smooth ducts with the previous results.

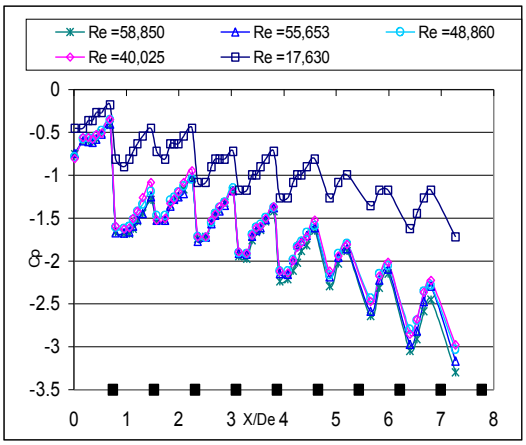

a) Bellmouth intake

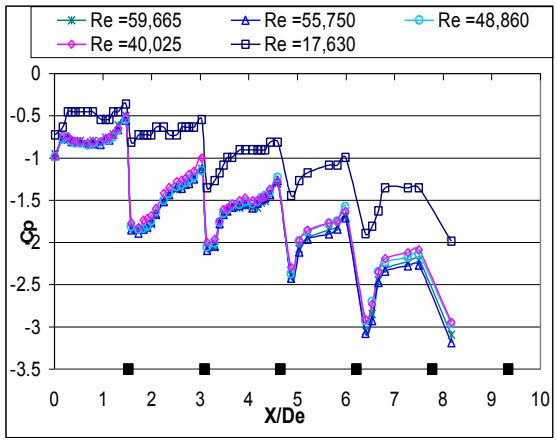

a) Bellmouth intake

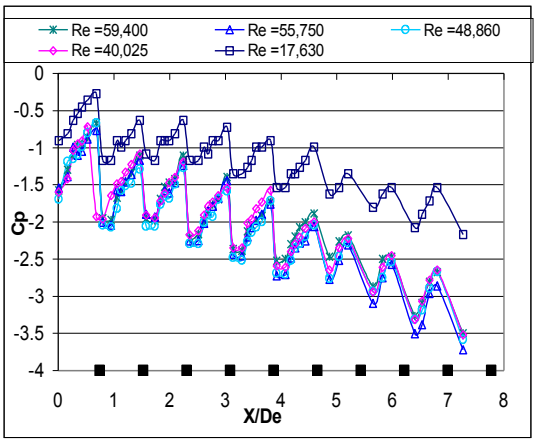

b) Plenum box intake

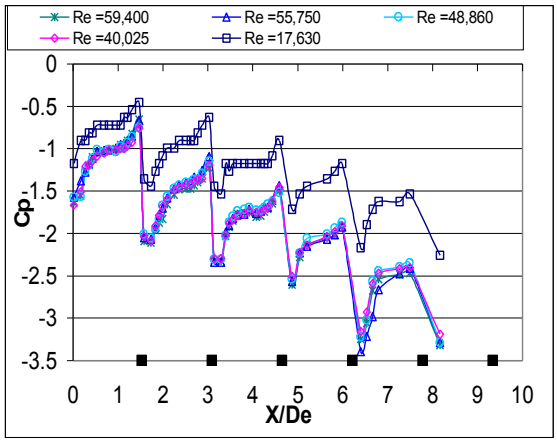

b) Plenum box intake

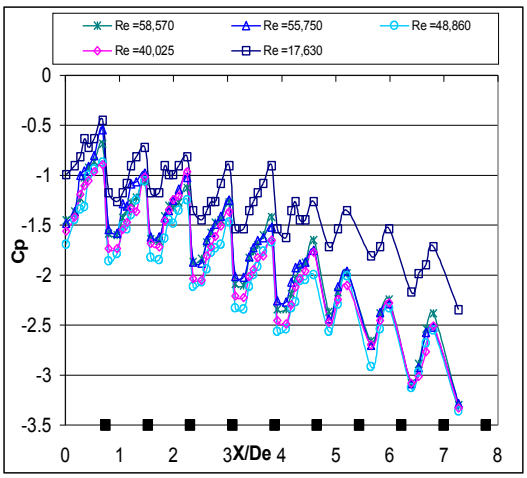

c) Abrupt intake

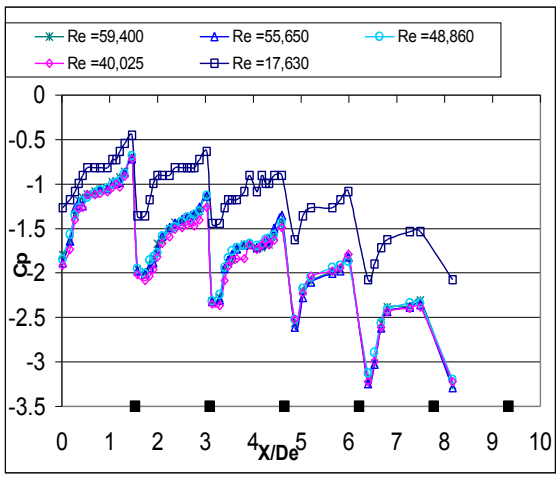

c) Abrupt intake

Fig(5) The local static pressure coefficient for square ribs (P/e=10) with different intake shapes at different Reynolds numbers.

Fig(6) The local static pressure coefficient for square ribs (P/e=20) with different intake shapes at different Reynolds numbers.

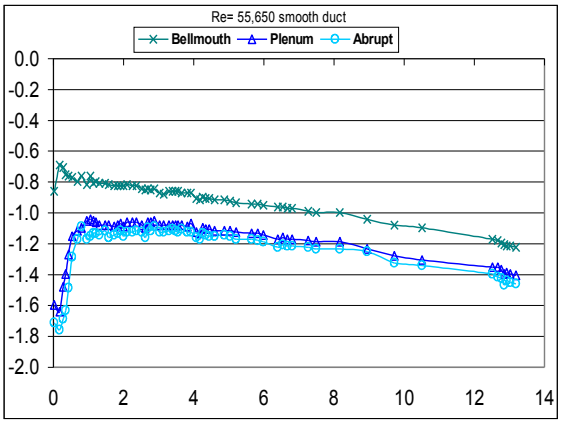

Fig(7) The static pressure coefficient axial distribution for smouth duct with different intakes shapes at Re=55,650.

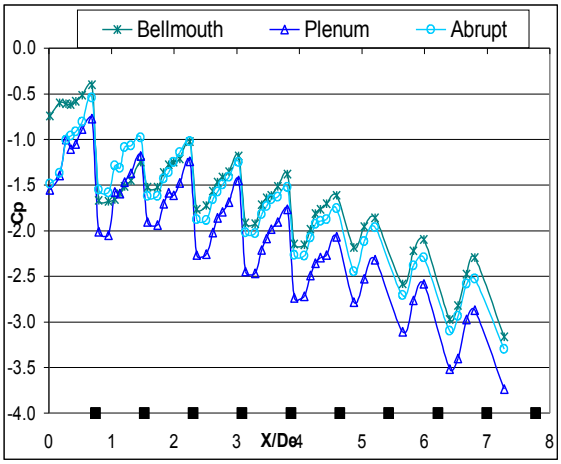

Fig(8) The static pressure coefficient axial distribution for ribbed duct with square ribs (P/e =10) with different intakes shapes at Re=55,650.

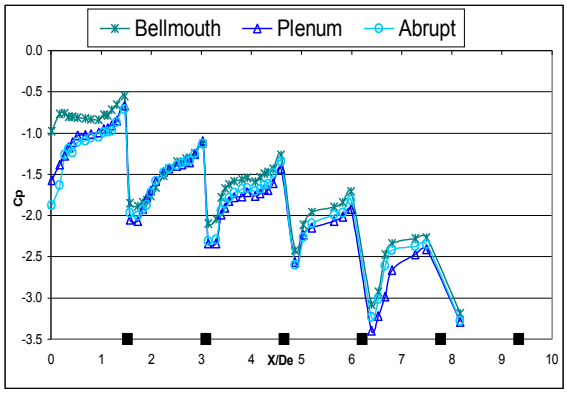

Fig(9) The static pressure coefficient axial distribution for ribbed duct with square ribs (P/e =20) with different intakes shapes at Re=55,650.

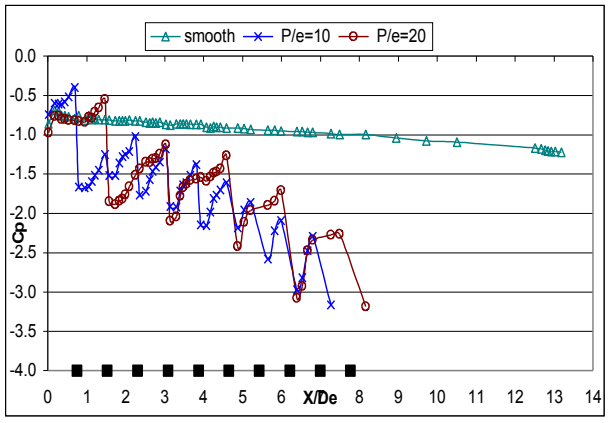

Fig(10) The static pressure coefficient axial distribution for duct with bellmouth intake ribbed with square ribs at different pitch to height ratios at Re=55,650.

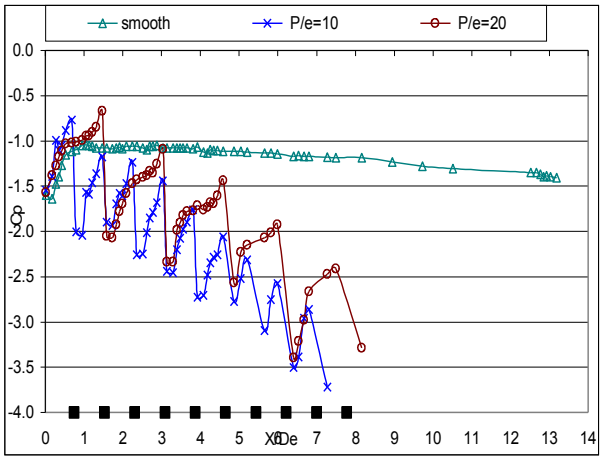

Fig(11) The static pressure coefficient axial distribution for duct with plenum intake ribbed with square ribs M85at different pitch to height ratios at Re=55,650.

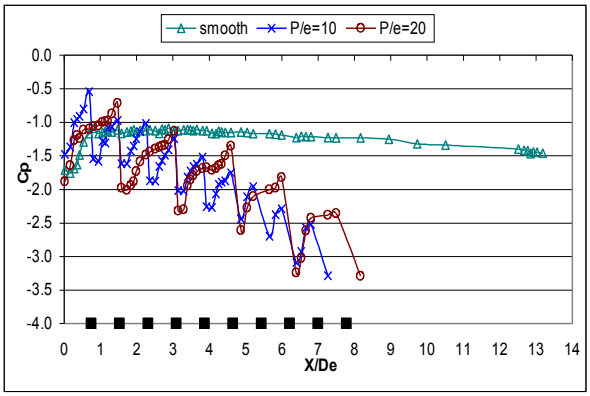

Fig(12) The static pressure coefficient axial distribution for duct with abrupt intake ribbed with square ribs at different pitch to height ratios at Re=55,650.

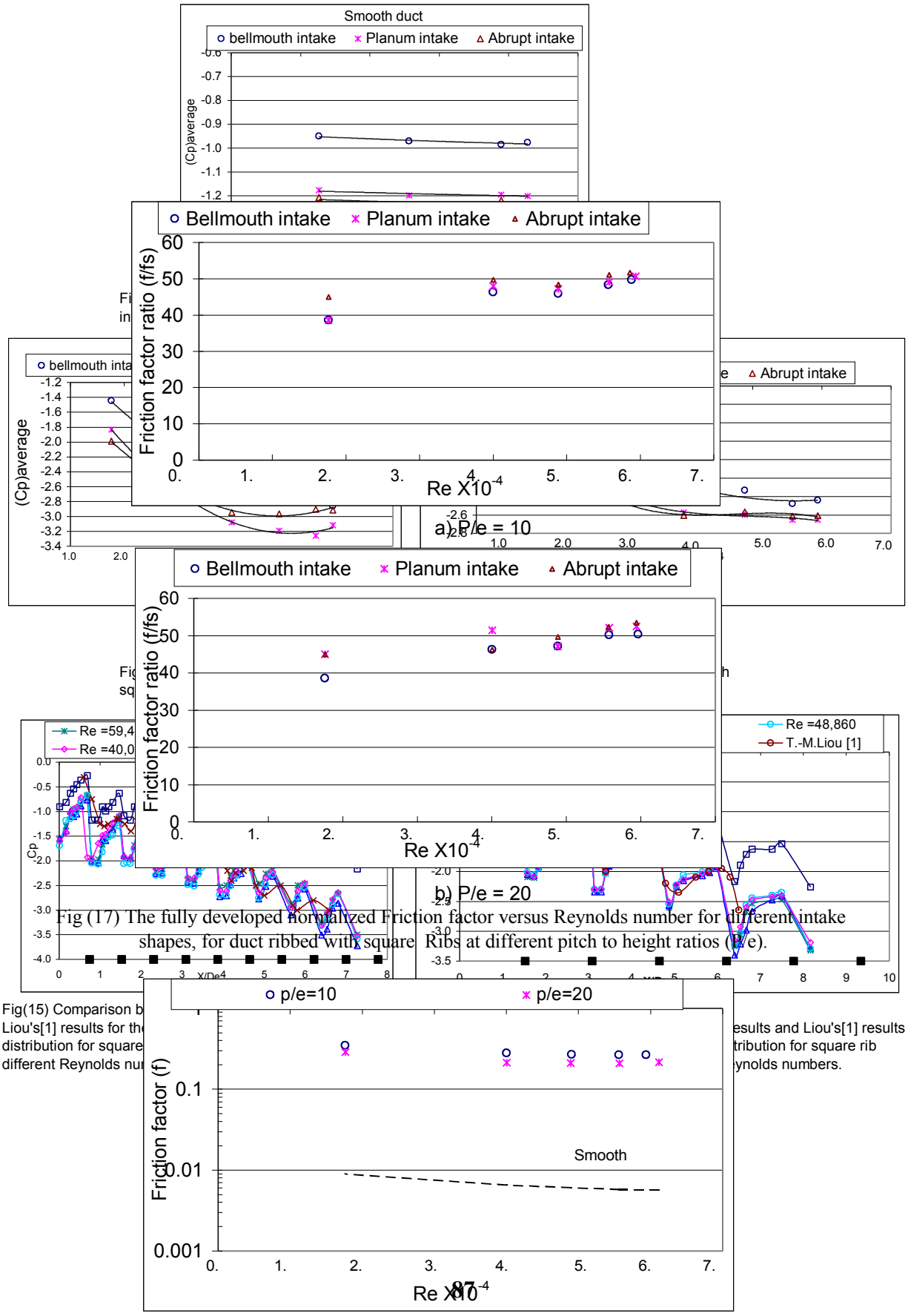

Fig (17) The fully developed normalized Friction factor versus Reynolds number for different intake shapes, for duct ribbed with square Ribs at different pitch to height ratios (P/e).

Fig. (18) The fully developed Friction factor versus Reynolds number for a duct ribbed with square ribs at different pitch to

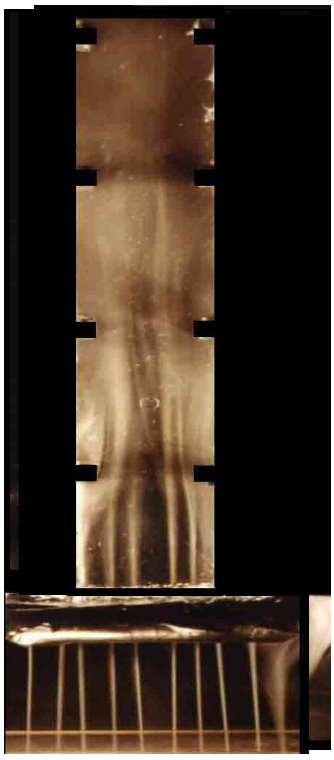

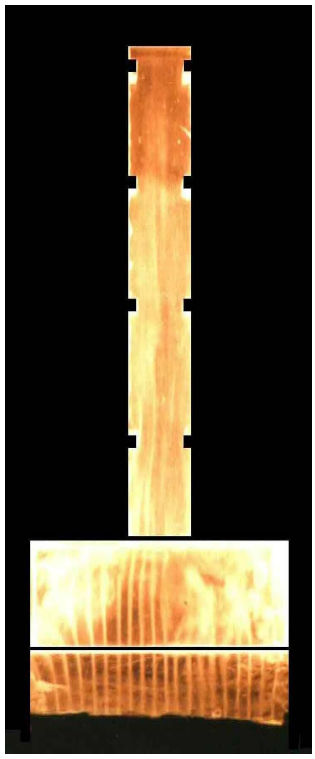

(a) bellmouth (b) Abrupt intake c) plenum intake)

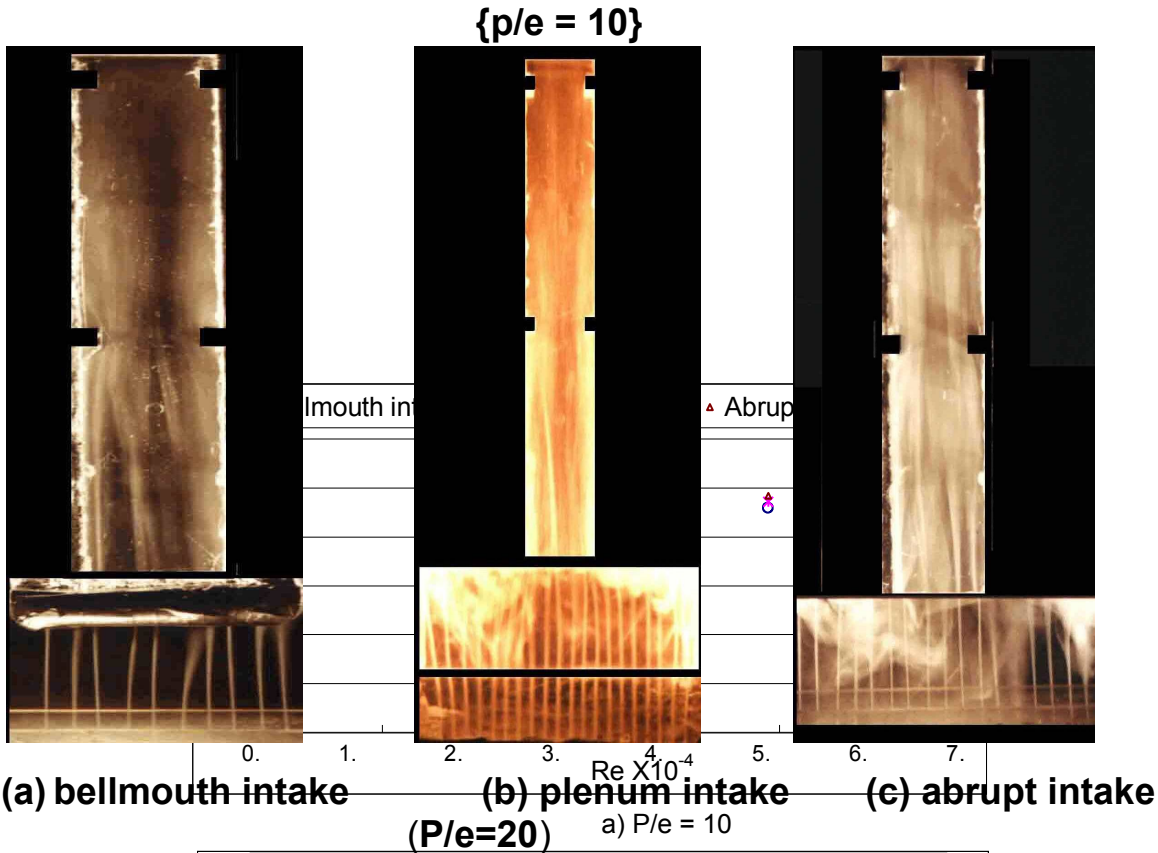

Fig.(19) Flow visualization for square ribbed duct at (e/H = 0.125) with different intake shapes

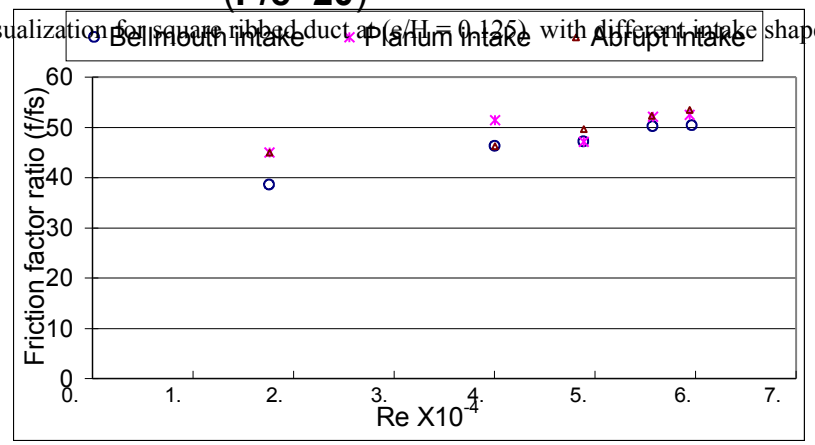

a) P/e = 10

b) P/e = 20

Fig (17) The fully developed normalized Friction factor versus Reynolds number for different intake shapes, for duct ribbed with square Ribs at different pitch to height ratios (P/e).

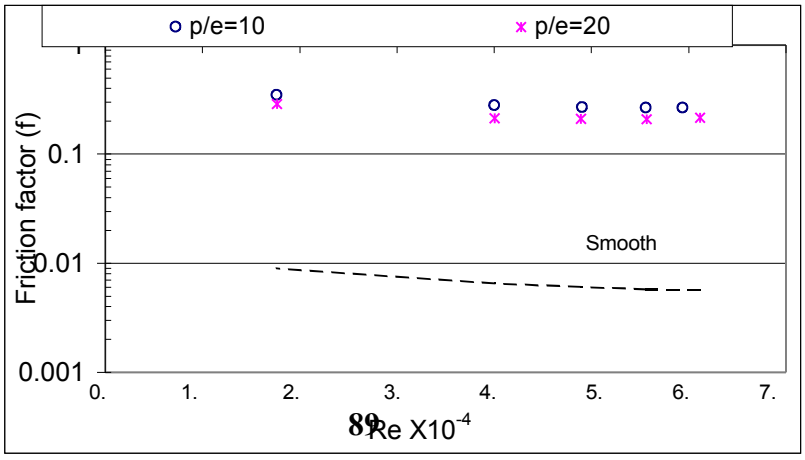

Fig. (18) The fully developed Friction factor versus Reynolds number for a duct ribbed with square ribs at different pitch to